NANOSYSTEMS:
PHYSICS, CHEMISTRY, MATHEMATICS

Garanin F.E., et al. *Nanosystems: Phys. Chem. Math.*, 2026, **17** (1), 34–38.
http://nanojournal.ifmo.ru
DOI 10.17586/2220-8054-2026-17-1-34-38

Original article

Spin wave propagation in a cross-shaped microwave guides made of yttrium iron garnet film with magnetic cylinders

Fedor E. Garanin[1,a], Alexander V. Sadovnikov[1,b], Maria V. Lomova[1,c]

[1]Saratov State University, Saratov, Russia

[a]garaninfedorwork@mail.ru, [b]sadovnikovav@gmail.com, [c]lomovamv85@mail.ru

Corresponding author: F. E. Garanin, garaninfedorwork@mail.ru

ABSTRACT This study explores the application of spin waves for developing functional components for information processing, transmission, and storage within the microwave and terahertz frequency regimes. The platform is based on yttrium iron garnet thin films, with spin wave manipulation achieved via two-dimensional arrays of magnetite cylinders. A numerical micromagnetic analysis of a cross-shaped waveguide was conducted by solving the Landau-Lifshitz-Gilbert equation, examining the dependence of wave properties on the orientation of the external magnetic field. The findings indicate a viable pathway toward the realization of compact and energy-efficient magnonic devices.

KEYWORDS numerical micromagnetic modeling, yttrium iron garnet, magnetic cylinders, spin wave.

ACKNOWLEDGEMENTS This work was supported by the Russian Science Foundation (Project No. 23-13-00373).

FOR CITATION Garanin F.E., Sadovnikov A.V., Lomova M.V. Spin wave propagation in a cross-shaped microwave guides made of yttrium iron garnet film with magnetic cylinders. *Nanosystems: Phys. Chem. Math.*, 2026, **17** (1), 34–38.

1. Introduction

Magnonics [1] is a rapidly evolving field of modern physics and nanotechnology that studies the transfer of magnetic moment or electron spin as an alternative to conventional charge transfer. This discipline opens new possibilities for creating information processing, transmission, and storage devices in the microwave and terahertz ranges [2, 3]. In such devices, the information signal is encoded in the phase or amplitude of a spin wave (SW), and logical operations are implemented based on the principles of spin-wave interference [2]. Spin waves represent collective oscillations of magnetic moment orientations in magnetically ordered materials, which can be used to encode information through phase modulation.

One of the key materials for creating magnetic waveguiding structures is yttrium iron garnet (YIG), which exhibits record-low spin wave damping even at nanoscale thicknesses [1].

Control of spin waves is one of the key challenges in magnonics. One approach to solving it involves the use of two-dimensional arrays of magnetic nanostructures, particularly magnetite cylinders, which are responsible for the modification of SW dispersion characteristics and the control of their propagation. In our previous studies, we investigated rectangular YIG waveguides functionalized with magnetite of varying geometry [4–6]. These works demonstrated effective manipulation of spin-wave transmission, but were limited to single-channel geometries with only one output port, thereby restricting the ability to control the spatial distribution of the signal.

This work presents a numerical micromagnetic simulation of a cross-shaped YIG waveguide with a two-dimensional array of magnetite cylinders, featuring three output ports ($P_{out\_1,2,3}$). We demonstrate that changing the direction of the external magnetic field along or opposite to the OY axis not only modulates the amplitude of the transmitted signal but also redistributes the spin-wave energy among the output channels. This directional control, enabled by the inhomogeneous internal magnetic field induced by the magnetite array, opens new pathways toward the realization of compact, multiport, and energy-efficient magnonic devices capable of spatial signal routing.

2. Method

The considered structure is a cross-shaped waveguide with an array of cylinders on its surface (see Fig. 1). The microwave waveguide is made from a YIG film ($Y_3Fe_5O_{12}$) with a length of $L = 4$ mm, a width of $W = 500$ μm, and a thickness of 10 μm. The cylinders were made of magnetite (Fe_3O_4), each with a diameter and height of 10 μm. The array of cylinders was positioned in a 500 μm$\times$500 μm area located at the center of the structure. The distance between the centers of the cylinders, both vertically and horizontally, was $d = 10$ μm. This area contained an array of 25$\times$25 cylinders (number along OX$\times$OY). The ends of the structure feature exciting and receiving antennas, labeled P_{in} and P_{out_1}, P_{out_2}, P_{out_3}, respectively. The antennas have dimensions of 30 μm$\times$500 μm.

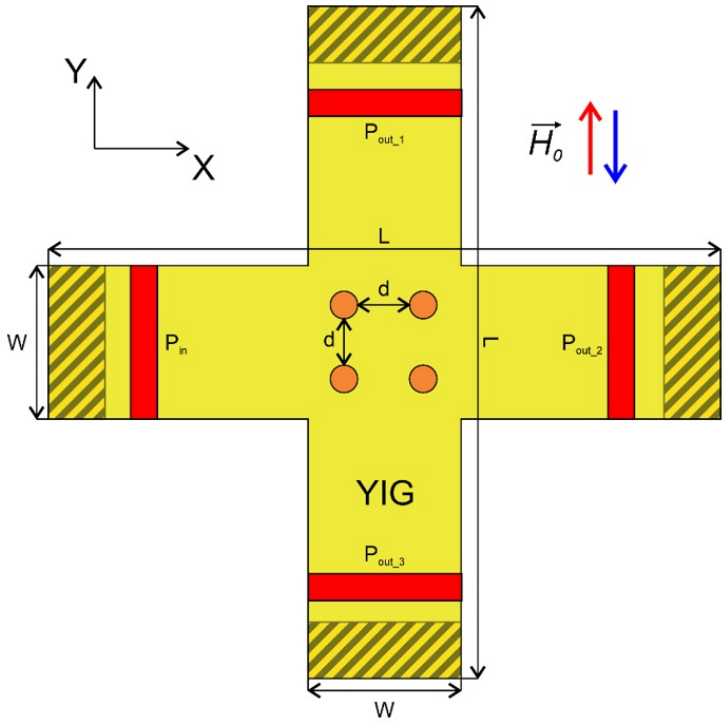

FIG. 1. Schematic illustration of the cross-shaped structure with an array of magnetite cylinders

Using micromagnetic modeling based on solving the Landau-Lifshitz-Gilbert (LLG) equation [7], a study of spin wave propagation modes in the structure (see Fig. 1) was conducted. The LLG equation can be represented as:

$$\frac{\partial \mathbf{M}}{\partial t} = \gamma \left[\mathbf{H}_{\mathbf{e}ff} \times \mathbf{M}\right] + \frac{\alpha}{M_0}\left[\mathbf{M} \times \frac{\partial \mathbf{M}}{\partial t}\right]. \quad (1)$$

Here $\mathbf{M}$ is the magnetization vector, α is the damping parameter, $\mathbf{H}_{\mathbf{e}ff} = \mathbf{H_0} + \mathbf{H}_{\mathbf{d}emag} + \mathbf{H}_{\mathbf{e}x}$ is the effective magnetic field, $\mathbf{H_0}$ is the external magnetic field, $\mathbf{H}_{\mathbf{d}emag}$ is the demagnetization field, $\mathbf{H}_{\mathbf{e}x}$ is the exchange field, and $\gamma = 2.8$ MHz/Oe is the gyromagnetic ratio.

The damping parameters for the YIG film and magnetite are $5{\times}10^{-4}$ and $2{\times}10^{-2}$, respectively. The exchange constant in the YIG film is $A_{ex1} = 3.612$ pJ/m, and in magnetite, it is $A_{ex2} = 1.210$ pJ/m. The saturation magnetizations of YIG and magnetite are $4\pi M_{YIG} = 1750$ G and $4\pi M_{Mag} = 6000$ G, respectively. The structure was placed in a uniform static magnetic field of $H_0 = 1200$ Oe. Cases involving the excitation of surface magnetostatic waves (SMW) were considered. In these cases, the external magnetic field $\mathbf{H_0}$ was applied along and opposite direction of the OY axis.

In the numerical simulation impulse excitation were used. For impulse excitation of SWs, a magnetic field $h_z(t) = h_0 \sin c(2\pi f_m t)$ was applied to the YIG film in the region of the input antenna P_{in}, where the central frequency $f_m = 6$ GHz, $h_0 = 0.001$ Oe. The value of the dynamic magnetization $M_z(x, y, t)$ was recorded in the regions of the receiving antennas P_{out_1}, P_{out_2}, P_{out_3} with a time step of $\Delta t = 20$ ps over a period of $T = 300$ ns, which is sufficient to reach a steady state.The mesh cell size was $2{\times}2{\times}2$ μm^3. The values of $m_z(x, y, t)$ were calculated for all cells using the formula $m_z(x, y, t) = M_z(x, y, t) - M_z(x, y, 0)$, where $M_z(x, y, 0)$ corresponds to the ferromagnetic state. To reduce spin wave reflections from the boundaries of the computational domain, absorbing layers with a geometrically increasing damping coefficient α were introduced (hatched areas in Fig. 1) [8, 9]. This approach was used to create time dependencies of the magnetization $m_z(x, y, t)$, which were then analyzed using the Fast Fourier Transform [10] to obtain amplitude-frequency characteristics (AFC).

3. Results and discussion

The internal demagnetization fields in the structure were calculated for different directions of $\mathbf{H_0}$. Fig. 2 shows the distribution of the internal field in the YIG film with magnetite. It can be observed that the magnetite introduces inhomogeneity into the internal field of the YIG film.

To obtain information about what happened to the wave after interacting with the magnetite array, the spectral power density of the spin wave signal was calculated. Fig. 3 shows the AFC for the structure when varying the direction of the external magnetic field. The blue/red line corresponds to the external magnetic field directed along/opposite OY direction. The dark blue/brown line corresponds to the AFC for the YIG film without magnetite with $\mathbf{H_0}$ oriented along/opposite OY direction. The dark blue and brown curves in the passband region are qualitatively the same, which is why the dark

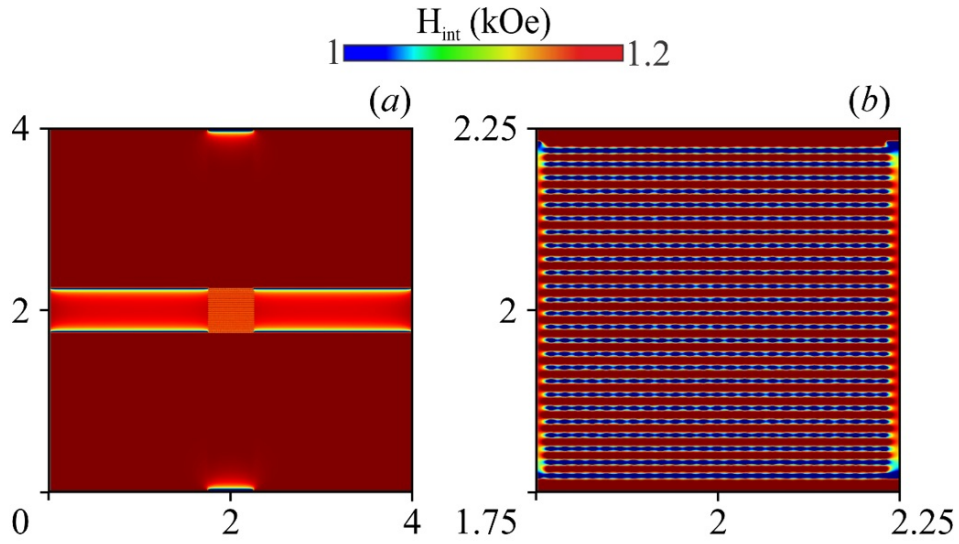

FIG. 2. A map of the internal magnetic field (H_{int}) distribution in the cross-shaped structure with an array of magnetite cylinders (a). A map of the H_{int} distribution, taken in the region where the array of magnetite cylinders is located (b)

blue curve is not visible in the AFC. Fig. 3a is plotted from data from antenna P_{out_1}, Fig. 3b from antenna P_{out_2}, and Fig. 3c from antenna P_{out_3}.

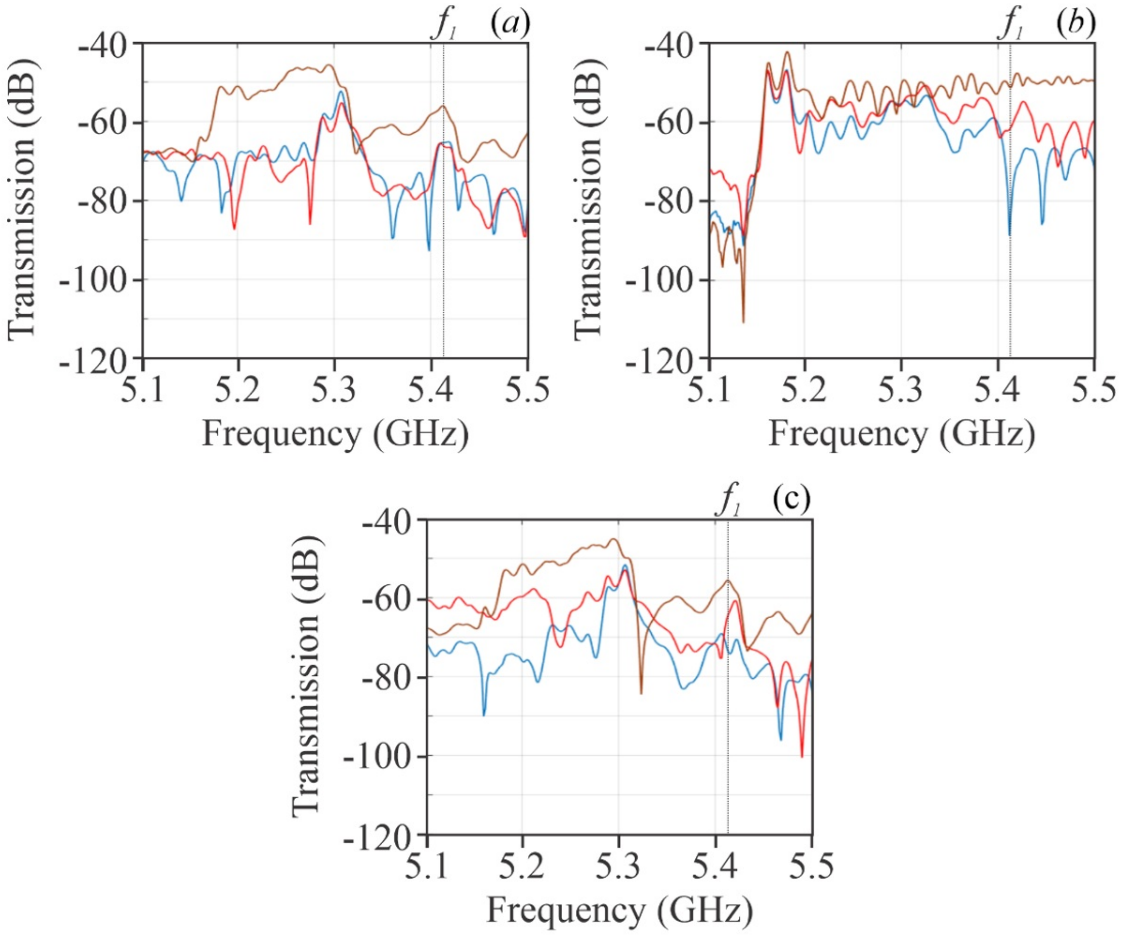

FIG. 3. Amplitude-frequency characteristics obtained for the output ports P_{out_1} (a), P_{out_2} (b), and port P_{out_3} (c)

The AFCs show that depositing magnetite onto the YIG film results in signal degradation regardless of whether the external magnetic field $\mathbf{H_0}$ is applied along or opposite to the OY axis. When changing the direction of $\mathbf{H_0}$, a specific frequency $f_1 = 5.415$ GHz can be identified (see Fig. 3b). The AFCs show that depositing magnetite onto the YIG film results in signal degradation regardless of whether the external magnetic field H_0 is applied along or opposite to the OY axis. When changing the direction of $\mathbf{H_0}$, a specific frequency $f_1 = 5.415$ GHz can be identified (see Fig. 3b). At this frequency, the transmission characteristics differ significantly depending on the field orientation. For an external field direction opposite to the OY axis (blue curve), a deep dip is observed at port P_{out_2} with a minimum transmission value of approximately -93 dB. For an external field direction along the OY axis (red curve), a significantly weaker dip is observed at the same port, with a minimum transmission value of approximately -62 dB. This means that the difference in signal amplitude between the two states at port P_{out_2} is approximately 31 dB, which corresponds to a power ratio of roughly 1.3×10^3.

Furthermore, this directional dependence is not limited to the main output port (P_{out_2}). At the same frequency f_1 in the upper port P_{out_1} (see Fig. 3a), the minimum transmission values are approximately -65 dB for $\mathbf{H_0}$ opposite to OY and -67 dB for $\mathbf{H_0}$ along OY, indicating a smaller but still observable difference ($\sim$2 dB). In the lower port P_{out_3} (see Fig. 3c), the minimum transmission values are approximately -65 dB for $\mathbf{H_0}$ opposite to Oy and -74 dB for $\mathbf{H_0}$ along OY, showing a more pronounced difference of $\sim$9 dB.

This spatially non-uniform response across the three output ports demonstrates that the reversal of the external magnetic field does not merely attenuate the signal, but actively redirects and redistributes the energy flow of the spin wave within the cross-shaped structure. The strongest control effect is observed along the primary axis of propagation (port P_{out_2}), while the transverse ports (P_{out_1} and P_{out_3}) exhibit a more complex, asymmetric response, likely due to interference and mode conversion effects induced by the magnetite array's inhomogeneous demagnetizing field. The observed effects are caused by the emergence of local inhomogeneities in the internal magnetic field within the YIG film, induced by the presence of the magnetite. The magnetite creates a spatially non-uniform demagnetizing field, which disrupts the magnetization uniformity in the structure and leads to the overall signal degradation.

4. Conclusion

This article investigates the control of spin wave propagation in a cross-shaped YIG microwave waveguide with a two-dimensional array of magnetite cylinders on its surface. Numerical micromagnetic modeling demonstrated the possibility of altering spin wave characteristics by varying the orientation of the external magnetic field. It was established that the direction of the external magnetic field influences the amplitude-frequency characteristics.

The results show that changing external conditions allows for the control of spin wave parameters, opening new possibilities for creating highly efficient magnonic devices. An important aspect of this research is the technical feasibility of such structures, enabled by modern micro- and nanolithography methods. Furthermore, magnetite, used as the material for the cylinders, possesses unique magnetic properties and a broad range of applications in biomedicine [11–14] and sensor technologies [15,16]. Its biocompatibility [17] and capacity for functionalization [12] make this material promising for developing sensors and devices used in the diagnosis and treatment of biological systems.

Thus, the presented results could find applications not only in the field of magnonics but also in related areas such as biomedical engineering and sensor technology, expanding the potential uses of spin waves and magnetic nanostructures.

References

[1] Gurevich A. *Magnetic Resonance in Ferrites and Antiferromagnets*. Nauka Publ., Moscow, 1973, 220 p.

[2] Stancil D.D., Prabhakar A. *Spin Waves: Theory and Applications*. Springer Publ., Berlin, 2009, 348 p.

[3] Wang Q., Kewenig M., Schneider M., Verba R., Kohl F., Heinz B., Geilen M., Mohseni M., Lägel B., Ciubotaru F., Adelmann C., Dubs C., Cotofana S.D., Dobrovolskiy O.V., Brächer T., Pirro P., Chumak A.V. A magnonic directional coupler for integrated magnonic half-adders. *Nat. Electron.*, 2020, **3**, P. 765.

[4] Garanin F.E., Khutieva A.B., Lomova M.V., Sadovnikov A.V. Control of spin wave properties in bioactive systems based on YIG metasurfaces/ordered polymer films with magnetic microreservoirs. *Fizika Tverdogo Tela*, 2024, **66**(9), P. 1527–1534.

[5] Khutieva A.B., Sadovnikov A.V., Garanin F.E. [et al.] Spin wave propagation in YIG waveguides with magnetic microvolcanoes: Experiment and simulation. *Applied Physics Letters*, 2025, **126**(6), P. 062402.

[6] Garanin F.E., Khutieva A.B., Lomova M.V., Sadovnikov A.V. Upravlenie rasprostraneniem spinovykh voln v mikrovolnovode s dvumernym massivom magnitnykh mikrochastits razlichnoy geometrii. *Izvestiya Saratovskogo universiteta*. Novayaseriya Seriya: Fizika, 2025, **25**(1), P. 4–11. [In Russian]

[7] Vansteenkiste A., Leliaert J., Dvornik M., Helsen M., Garcia-Sanchez F., Waeyenberge B. The design and verification of MuMax3. *AIP Adv.*, 2014, **4**, P. 107133.

[8] Venkat G., Fangohr H., Prabhakar A. Absorbing boundary layers for spin wave micromagnetics. *J. Magn. Magn. Mater.*, 2018, **450**, P. 34.

[9] Dvornik M., Kuchko A.N., Kruglyak V.V. Micromagnetic method of s-parameter characterization of magnonic devices. *J. Appl. Phys.*, 2011, **109**, P. 07D350.

[10] Hu J., Jia F., Liu W. Application of Fast Fourier Transform. *HSET*, 2023, **38**, P. 590.

[11] Bustamante-Torres M., Romero-Fierro D., Estrella-Nuñez J., Arcentales-Vera B., Chichande-Proaño E., Bucio E. Polymeric Composite of Magnetite Iron Oxide Nanoparticles and Their Application in Biomedicine: A Review. *Polymers*, 2022, **14**, P. 752.

[12] Ganapathe L.S., Mohamed M.A., Mohamad Yunus R., Berhanuddin D. D. Magnetite (Fe_3O_4) Nanoparticles in Biomedical Application: From Synthesis to Surface Functionalisation. *Magnetochemistry*, 2020, **6**, P. 68.

[13] Włodarczyk A., Gorgoń S., Radoń A., Bajdak-Rusinek K. Magnetite Nanoparticles in Magnetic Hyperthermia and Cancer Therapies: Challenges and Perspectives. *Nanomaterials*, 2022, **12**, P. 1807.
[14] Petrov K.D., Chubarov A.S. Magnetite Nanoparticles for Biomedical Applications. *Encyclopedia*, 2022, **2**, P. 1811.
[15] Bilgic A., Cimen A. Two Novel BODIPY-Functional Magnetite Fluorescent Nano-Sensors for Detecting of Cr(VI) Ions in Aqueous Solutions. *J. Fluoresc.*, 2020, **30**, P. 867.
[16] Bilgic A., Cimen A. A highly sensitive and selective ON-OFF fluorescent sensor based on functionalized magnetite nanoparticles for detection of Cr(VI) metal ions in the aqueous medium. *J. Mol. Liq.*, 2020, **312**, P. 113398.
[17] Mbeh D.A., França R., Merhi Y., Zhang X.F., Veres T., Sacher E., Yahia L. In vitro biocompatibility assessment of functionalized magnetite nanoparticles: Biological and cytotoxicological effects. *J. Biomed. Mater. Res. Part A*, 2012, 100A, P. 1637.

Submitted 11 November 2025; accepted 1 December 2025

Information about the authors:

Fedor E. Garanin – Saratov State University, Saratov, Russia; ORCID 0009-0001-4999-2958; garaninfedorwork@mail.ru

Alexander V. Sadovnikov – Saratov State University, Saratov, Russia; ORCID 0000-0002-8847-2621; sadovnikovav@gmail.com

Maria V. Lomova – Saratov State University, Saratov, Russia; ORCID 0000-0002-7464-1754; lomovamv85@mail.ru

Conflict of interest: the authors declare no conflict of interest.